Neurobiology of Disease

Peroxisome Injury in Multiple Sclerosis: Protective Effects of 4-Phenylbutyrate in CNS-Associated Macrophages

Andrej Roczkowsky,[1] Matthew A.L. Doan,[6] Brittyne A. Hlavay,[1] Manmeet K. Mamik,[1] William G. Branton,[1] Brienne A. McKenzie,[5] Leina B. Saito,[5] Laura Schmitt,[2] Gary Eitzen,[3] Francesca Di Cara,[7] Melinda Wuest,[4] Frank Wuest,[4] Richard Rachubinski,[3] and Christopher Power[1,5,6]

[1]Departments of Medicine, [2]Laboratory Medicine & Pathology, [3]Cell Biology, [4]Oncology, [5]Medical Microbiology & Immunology, [6]The Neuroscience and Mental Health Institute, University of Alberta, Edmonton, Alberta T6G 2R3, Canada, and [7]Department of Microbiology & Immunology, Dalhousie University, Halifax, Nova Scotia B3H 4R2, Canada

Multiple sclerosis (MS) is a progressive and inflammatory demyelinating disease of the CNS. Peroxisomes perform critical functions that contribute to CNS homeostasis. We investigated peroxisome injury and mitigating effects of peroxisome-restorative therapy on inflammatory demyelination in models of MS. Human autopsied CNS tissues (male and female), human cell cultures, and cuprizone-mediated demyelination mice (female) were examined by RT-PCR, Western blotting, and immunolabeling. The therapeutic peroxisome proliferator, 4-phenylbutyrate (4-PBA) was investigated *in vitro* and *in vivo*. White matter from MS patients showed reduced peroxisomal transcript and protein levels, including PMP70, compared with non-MS controls. Cultured human neural cells revealed that human microglia contained abundant peroxisomal proteins. TNF-α-exposed microglia displayed reduced immunolabeling of peroxisomal proteins, PMP70 and PEX11β, which was prevented with 4-PBA. In human myeloid cells exposed to TNF-α or nigericin, suppression of PEX11β and catalase protein levels were observed to be dependent on NLRP3 expression. Hindbrains from cuprizone-exposed mice showed reduced *Abcd1*, *Cat*, and *Pex5l* transcript levels, with concurrent increased *Nlrp3* and *Il1b* transcript levels, which was abrogated by 4-PBA. In the central corpus callosum, Iba-1 in CNS-associated macrophages and peroxisomal thiolase immunostaining after cuprizone exposure was increased by 4-PBA. 4-PBA prevented decreased myelin basic protein and neurofilament heavy chain immunoreactivity caused by cuprizone exposure. Cuprizone-induced neurobehavioral deficits were improved by 4-PBA treatment. Peroxisome injury in CNS-associated macrophages contributed to neuroinflammation and demyelination that was prevented by 4-PBA treatment. A peroxisome-targeted therapy might be valuable for treating inflammatory demyelination and neurodegeneration in MS.

Key words: 4-phenylbutyrate; microglia; multiple sclerosis; neuroinflammation; peroxisome

---

Significance Statement

Multiple sclerosis (MS) is a common and disabling disorder of the CNS with no curative therapies for its progressive form. The present studies implicate peroxisome impairment in CNS-associated macrophages (CAMs), which include resident microglia and blood-derived macrophages, as an important contributor to inflammatory demyelination and neuroaxonal injury in MS. We also show that the inflammasome molecule NLRP3 is associated with peroxisome injury *in vitro* and *in vivo*, especially in CAMs. Treatment with the peroxisome proliferator 4-phenylbutyrate exerted protective effects with improved molecular, morphologic, and neurobehavioral outcomes that were associated with a neuroprotective CAM phenotype. These findings offer novel insights into the contribution of peroxisome injury in MS together with preclinical testing of a rational therapy for MS.

Introduction

Multiple sclerosis (MS) is a chronic inflammatory disease of the CNS characterized by advancing demyelination in the brain and spinal cord that is accompanied by neuro-axonal injury (Filippi et al., 2018). Progressive MS is the leading cause of nontraumatic disability in young adults and is currently incurable. The pathogenesis of MS involves breakdown of the blood–brain barrier, infiltration of leukocytes into the CNS, and activation of glia, including CNS-associated macrophages (CAMs) comprised of resident microglia and trafficking macrophages

Table 1. Clinical features of MS and non-MS patients[a]

	MS ($n = 23$)	Non-MS ($n = 18$)	p
Mean age (range, yr)	56 (25-77)	66 (36-89)	NS
M:F	11:12	9:9	NS
Disease phenotype	PP-MS ($n = 5$)	Non-CNS disease (cancer, sepsis, myocardial infarction, drug	
	RR-MS ($n = 4$)	overdose ($n = 12$), amyotrophic lateral sclerosis ($n = 3$), stroke ($n = 3$),	
	SP-MS ($n = 14$)	multisystem atrophy ($n = 1$)	
EDSS	4.0-9.5	NA	

[a]Mean age, sex, disease phenotype, and Expanded Disability Status Scale (EDSS) of MS ($n = 23$) and non-MS ($n = 18$) used in the present study. MS patients include primary progressive MS (PP-MS, $n = 5$), relapsing-remitting MS (RR-MS, $n = 4$), and secondary progressive MS (SP-MS, $n = 14$). Mann–Whitney U test was used to assess significant difference in age between MS and non-MS, and Fisher's exact test was used to assess significant difference in sex between groups.

as well as astrocytes that results in oligodendrocyte injury and death accompanied by demyelination and axonal loss (Hemmer et al., 2015).

Peroxisomes are membrane-bounded organelles that perform vital metabolic functions in the CNS, including the production of ether phospholipids that are critical for the formation and maintenance of myelin (Kassmann, 2014; Berger et al., 2016). Recently, there has been increased appreciation for peroxisomal activity in cells of myeloid origin in the context of infection and other disorders, in part, because of peroxisomal contributions to β-oxidation and modulation of Type 1 interferon responses (Di Cara et al., 2019). The cellular abundance of peroxisomes is controlled, in part, by peroxisome biogenesis factors called peroxins encoded by the *PEX* genes, of which there are 14 in humans (Smith and Aitchison, 2013; Farré et al., 2019).

Peroxisomes also serve as immunomodulatory hubs for innate immunity and mediate both pro- and anti-inflammatory responses (Di Cara et al., 2019). They are critical regulators of host immune responses to bacterial and viral infections through the nuclear factor κ-light chain-enhancer of activated B cells (Di Cara et al., 2017) and mitochondrial antiviral signaling adaptor pathways (Dixit et al., 2010), respectively. In contrast, greater peroxisome abundance in murine macrophages treated with the peroxisome proliferator 4-phenylbutyrate (4-PBA) reduced the induction of pro-inflammatory molecules, including TNF-α and cyclooxygenase-2, in response to challenge with LPS (Vijayan et al., 2017). Furthermore, peroxisome-derived long-chain polyunsaturated fatty acids such as eicosapentaenoic acid and docosahexaenoic acid have anti-inflammatory and pro-inflammatory-resolving properties in monocytes (Jaudszus et al., 2013) and microglia (Hjorth and Freund-Levi, 2012).

Due in part to its high metabolic demand and vulnerability to reactive oxygen species (ROS), the CNS is highly susceptible to peroxisome dysfunction (Uzor et al., 2020). In mice, CNS-specific KO of *PEX5*, which is critical for import of proteins into peroxisomes, resulted in impaired motor function, axonal injury, and demyelination in the corpus callosum (Hulshagen et al., 2008). Likewise, CNS-specific ablation of *PEX13* in mice caused impaired neurogenesis, gliosis, and cell death (Rahim et al., 2018). In humans, defects in *PEX* genes cause the peroxisome biogenesis disorders, which are associated with specific neurologic syndromes, including seizures and loss of vision and hearing (Berger et al., 2016). Peroxisomal dysfunction is implicated in several diseases of the CNS, including Alzheimer's disease and MS (Santos et al., 2005; Gray et al., 2014).

In the last decade, activation of pro-inflammatory protein complexes, called inflammasomes, has also been demonstrated to contribute to the pathogenesis of MS lesions (Barclay and Shinohara, 2017; McKenzie et al., 2018). Upon inflammasome activation, the pore-forming molecule gasdermin D (GSDMD) is cleaved to its active form by caspase-1, leading to release of pro-inflammatory cytokines IL-1β and IL-18 and an inflammatory form of regulated cell death termed pyroptosis. Pharmacological targeting of the NOD-like receptor protein 3 (NLRP3) inflammasome or inhibition of caspase-1 reduced disease severity in the mouse autoimmune encephalomyelitis model of MS (Coll et al., 2015; McKenzie et al., 2018; Malhotra et al., 2020). Nonetheless, a link between peroxisome function and inflammasome activation has not been previously investigated.

Here, we investigated the role of peroxisome dysfunction in MS and its relationship to inflammasome activation. We found decreased peroxisomal gene expression and decreased amounts of peroxisomal proteins in subcortical white matter of MS patients, in primary cultured microglia exposed to inflammatory stimuli, and in CAMs in brains of cuprizone (CPZ)-exposed mice. These observations were associated with NLRP3 transcript upregulation in the CPZ model. KO of NLRP3 in a human monocytic cell line prevented a decrease in critical peroxisomal proteins. Moreover, treatment of CPZ-exposed mice with the peroxisome proliferator 4-PBA improved neurobehavioral outcome, reduced demyelination and neuroaxonal injury, while also restoring levels of peroxisome gene expression.

Materials and Methods

Ethics statement. Human fetal tissues were obtained from 15-22 week aborted male and female fetuses that were collected with the written informed consent of the donor and approved by the University of Alberta Human Research Ethics Board (Biomedical) (Pro00027660). The use of autopsied brain tissues was approved (Pro0002291) by the University of Alberta Human Research Ethics Board (Biomedical), and written informed consent was received for all samples. Cerebral frontal white matter (normal appearing white matter only) from MS patients and other disease controls (non-MS) were examined (Table 1). All animals were housed and monitored on a regular schedule, and experiments were performed according to the Canadian Council on Animal Care and University of Alberta Health Sciences Animal Care and Use Committee guidelines. All data from these studies will be made available on request.

Cell cultures. Primary fetal human microglia were isolated based on differential culture conditions, as previously described (Mamik et al., 2016, 2017). Fetal brain tissues from 17-20 week fetuses were dissected, meninges were removed, and a single-cell suspension was produced through enzymatic digestion for 60 min with 2.5% trypsin and 0.2 mg DNase I/ml, followed by trituration through a 70 µm cell strainer. Cells were washed twice with fresh medium and plated in T-75 flasks. Cultures were maintained in MEM supplemented with 10% FBS, 2 mM L-glutamine, 1 mM sodium pyruvate, 1 × MEM nonessential amino acids, 0.1% dextrose, 100 U penicillin/ml, 100 µg streptomycin/ml, 0.5 µg amphotericin B/ml, and 20 µg gentamicin/ml. For microglial cells, mixed cultures were maintained for 1-2 weeks, at which point astrocytes and neurons formed an adherent cell layer, with microglia loosely attached or free floating in the medium. Cultures were gently rocked for 20 min to resuspend the weakly adhering microglia in

medium, which were then decanted, washed, and plated. Purity of cultures was verified by immunofluorescence as reported (Walsh et al., 2014).

MO3.13 cell cultures (CELLutions) were maintained in DMEM supplemented with 10% FBS containing 100 U penicillin/ml and 100 μg streptomycin/ml. Before experimentation, cells were differentiated for 3 d using PMA (100 nM) in serum-free DMEM before medium was removed, cells were washed with PBS, and fresh medium (serum-free) was added for future experimentation.

GSDMD, NLRP3, and mock THP-1 KO cell lines were generated using CRISPR-Cas9 as described previously (Platnich et al., 2018). All THP-1 cell lines were cultured in RPMI with 10% FBS, 2 mM L-glutamine, 0.05 mM 2-mercaptoethanol, 1 mM sodium pyruvate, 100 U penicillin/ml, and 100 μg streptomycin/ml, as described previously (Walsh et al., 2014). To differentiate, cells were treated for 18 h with PMA (50 nM). Following PMA exposure, cells were washed once with PBS, and fresh medium without PMA was added to the cells. Cells were stimulated as described with TNF-α (50 ng/ml) (R&D Systems, 210-TA) for 24 h or nigericin (6.7 μM) (Invivogen) for 4 h with appropriate vehicle controls. Cells were either harvested in TRIzol reagent (Invitrogen) for subsequent RNA isolation or protein analysis after detachment by 5 min incubation in TrypLE Express (Invitrogen, 12 605-028) and pelleted at $350 \times g$ for 5 min. Pellets were washed with PBS and lysed in $1 \times$ RIPA buffer (Abcam, ab156034) with protease inhibitor cocktail (EMD Millipore, 539134).

Immunoblot analyses. Immunoblot analysis of tissue and cell lysates was performed as described previously (Walsh et al., 2014; Boghozian et al., 2017). Following protein extraction using RIPA buffer, total protein was quantified using a DC Protein Assay Kit (Bio-Rad, 5000112), then dissolved in Laemmli buffer (Bio-Rad, 161-0747) and incubated at 95°C for 5 min. Samples were loaded onto 4%-20% precast SDS-PAGE gels (Bio-Rad, 456-1094) and run for 80 min at 120 V. Following electrophoresis, gels were transferred onto 0.2 μm nitrocellulose membranes (Bio-Rad, 1620112) using a Bio-Rad Mini Trans-Blot Wet Transfer system for 60 min at 100 V. Membranes were blocked for 2 h with 5% skim milk or 3% BSA (Sigma, A4503) in PBS with 0.1% Tween-20 (PBS-T), followed by overnight incubation with primary antibody at 4°C. Primary antibodies used for immunoblot, immunohistochemistry and immunofluorescence are provided in Extended Data Figure 1-1. Membranes were then washed 3×5 min with PBS-T and incubated with anti-rabbit or anti-mouse HRP-conjugated secondary antibody (1:500, Jackson ImmunoResearch Laboratories) for 2 h at room temperature, followed by 5 min washes ($3\times$) with PBS-T. Membranes were developed with ECL reagent (Thermo Fisher Scientific, 32132) and imaged using an ImageQuant LAS4000 Biomolecular Imager (GE Life Sciences). Densitometry analysis was performed using Image J software and normalized to β-actin band intensity.

Cell culture immunofluorescence. Detection of cellular proteins was performed using immunofluorescence as described previously (Walsh et al., 2014). Human fetal microglia cells were cultured on 180-μm-thick polymer coverslip 8-well plates (μ-Slide ibiTreat plates #80826) and treated with TNF-α (50 ng/ml-TA) with or without 4-PBA (100 μM) (Sigma SML0309) or with appropriate vehicle control for 24 h. After treatment, cells were fixed using 4% PFA. Cells were permeabilized using 0.1% Triton X-100 in PBS, blocked using Odyssey blocking buffer (LiCor, 927-40 000), and incubated with primary antibody overnight at 4°C. Slides were washed 15 min ($3\times$) with PBS, and primary antibody binding was detected using AlexaFluor-488 goat anti-rabbit IgG (1:500) (Abcam, ab150077) or AlexaFluor-568 goat anti-mouse IgG (1:500) (Abcam, ab175473). Cells were then washed 15 min ($3\times$), stained with DAPI for 10 min, washed again 3×15 min, and then mounted using Prolong Gold antifade reagent (Invitrogen, P36934). Slides were imaged using a Wave FX spinning disk confocal microscope (Carl Zeiss) with Volocity 6.3 acquisition and analysis software (PerkinElmer). Three channels were acquired sequentially by changing light paths and by moving stage upwards for 29 Z slices (0.35 μm per step).

Tissue immunofluorescence. Tissue slides were deparaffinized by incubation for 1 h at 60°C followed by one 10 min and two 5 min incubations in toluene baths through decreasing concentrations of ethanol to distilled water, as described previously (Boghozian et al., 2017). Antigen retrieval was performed by boiling in 10 mM sodium citrate, pH 6.0.

Slides were blocked with HHFH buffer (1 mM HEPES buffer, 2% (v/v) horse serum, 5% (v/v) FBS, 0.1% sodium azide in HBSS) for 4 h at room temperature. Slides were incubated with primary antibodies at 4°C overnight. Primary antibody was removed by 5 min ($3\times$) washes with PBS, and slides were incubated for 3 min in TrueBlack Lipofuscin autofluorescence quencher (Biotium, 23007) and then washed an additional 3 times in PBS. Slides were incubated in a mixture of 1:500 fluorescent secondary antibodies as appropriate for 2 h, stained with DAPI for 10 min, washed 3 times in PBS, and mounted with Prolong Gold. Slides were imaged with an inverted Wave FX spinning disk confocal microscope.

RT-PCR. One microgram of total RNA was used for first-strand cDNA synthesis using Superscript II reverse transcriptase (Invitrogen) and random hexamer primers (Roche). Specific genes were quantified by semiquantitative real-time polymerase chain reaction (RT-PCR) using the CFX 96 real-time system (Bio-Rad). The specific oligonucleotide primers used in RT-PCR are provided in Extended Data Figure 1-2. Semiquantitative RT-PCR analysis was performed by monitoring, in real time, the increase in fluorescence of the SYBR Green dye (iQ SYBR Green Supermix, Bio-Rad) measured on the Bio-Rad detection system (Maingat et al., 2013), which was expressed as relative fold change of transcripts of genes of interest normalized to GAPDH transcript and relative to untreated cells and other-disease controls.

CPZ exposure. Ten-week-old control female C57BL/6J mice (The Jackson Laboratory) were fed on Nutra-Gel diet (BioServ, F4798-KIT) for 6 weeks while the CPZ-exposed group received Nutra-Gel diet containing 0.265% CPZ (Sigma-Aldrich, 14 690) for 4 weeks starting on week 3 of the experiment. To assess the effect of 4-PBA in this model, 4-PBA (100 mg/kg) was administered intraperitoneally daily to mice (for 14 d) starting after 2 weeks of CPZ exposure and while maintaining them on the control or CPZ diets. At the end of the fourth week of CPZ exposure, mice were killed. Forebrain tissue was fixed in 4% PFA, and hindbrain tissue (cerebellum and brainstem) was flash frozen in liquid nitrogen. Hindbrain tissue was homogenized using FastPrep24 tissuelyser (MP Biomedicals), and RNA and protein were extracted using the AllPrep kit (QIAGEN) following the manufacturer's instructions. Protein pellets were resuspended in 5% SDS.

Immunohistochemistry. Tissue sections were deparaffinized for 1 h at 60°C, washed 2×5 min in toluene, and hydrated using decreasing concentrations of ethanol. Antigen retrieval was performed by boiling the slides in 0.01 M trisodium citrate buffer, pH 6.0, for 10 min. Endogenous peroxidases were inactivated by incubating sections in 0.3% hydrogen peroxide for 20 min. To prevent nonspecific binding, sections were pre-incubated with Odyssey buffer (LiCor, 927-40 000) for 3 h at room temperature before overnight incubation with primary antibody. Biotinylated secondary antibodies were applied for 2 h, and immunoreactivity was detected using the Vectastain Avidin-Biotin Complex (ABC) kit (Vector Laboratories, VECTPK6100) with a DAB peroxidase substrate kit (Vector Laboratories, SK-4100). All slides were imaged using an upright Axioskop2 microscope (Carl Zeiss).

Slides were imaged using an Axioskop 2 microscope in conjunction with QC Capture Pro 6.0 software. LFB-stained or DAB-immunopositive areas were measured with Image J FIJI (Schindelin et al., 2012), by adjusting for saturation and brightness to remove nonspecific artifacts, converting to a 16 bit format, selecting the corpus collosum using the *Freehand selections* tool, setting the *Threshold* maximum and minimum values at 85, and measuring the percent stained area that met those thresholds within the selected corpus callosum per animal. For percent unstained area, similar settings were used as above, except the *Color Threshold* tab was set to full range for hue and brightness, and the saturation was adjusted to select for anything that was not stained tissue.

Neurobehavioral testing. Analyses of anxiety- and motor-associated behaviors were performed at week 4 after CPZ exposure in mice as described previously (Mamik et al., 2017). The open field locomotion test was performed in a large $80 \times 70 \times 20$ cm plastic container. The container was sectioned into four equal quadrants and one central square ($224\ cm^2$). Each test was conducted for 5 min and began when the mouse was placed in the center of the field. The mouse was considered to have performed a "cross" when its entire body crossed into a new quadrant.
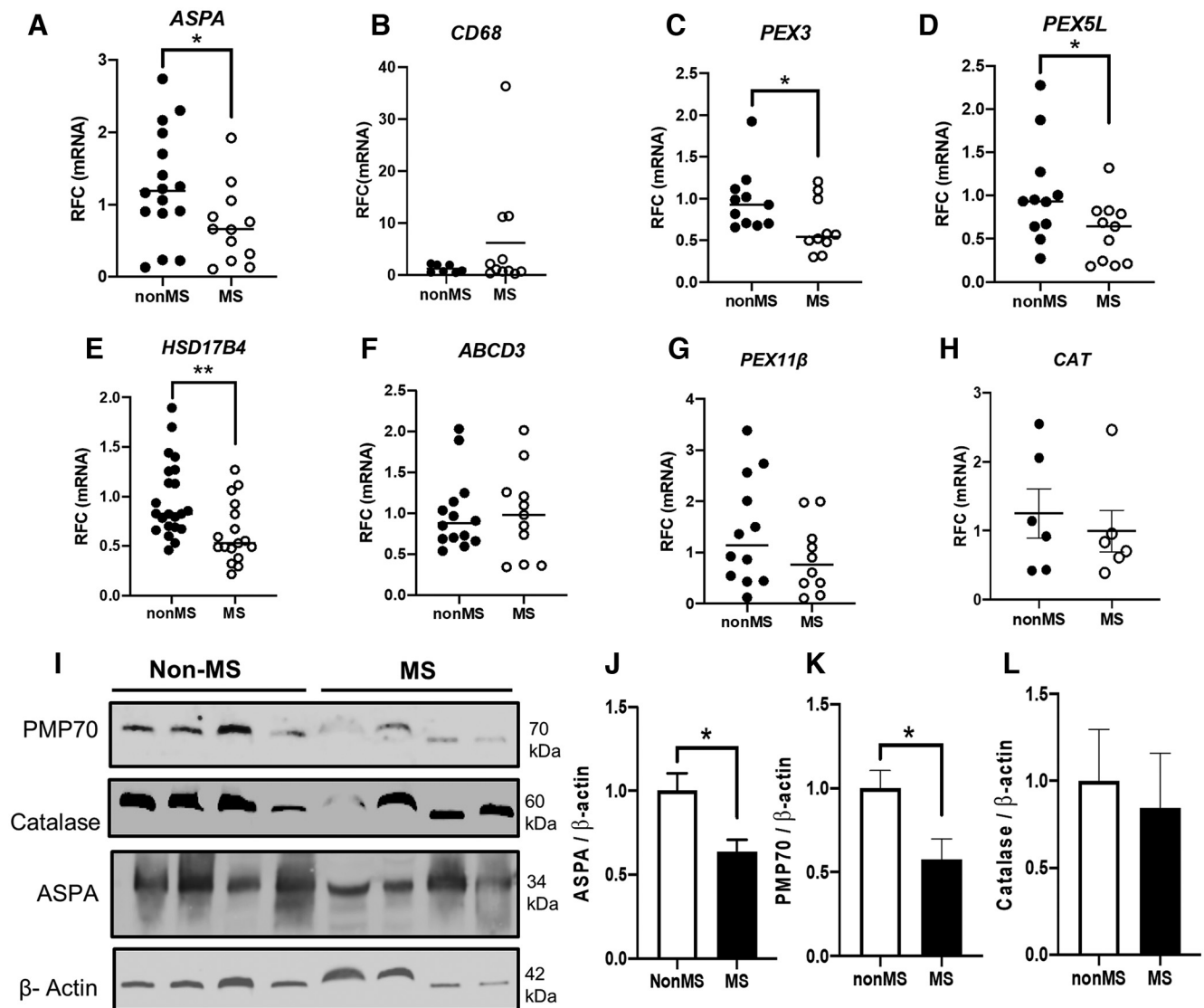
Figure 1. Peroxisome biogenesis and structural components are dysregulated at the transcript and protein levels in white matter of patients with MS. **A–H**, Autopsy normal-appearing subcortical white matter samples from patients with MS and non-MS (control) patients were analyzed by RT-PCR targeting select peroxisome and inflammation-related genes *ASPA* (**A**), *CD68* (**B**), *PEX3* (**C**), *PEX5L* (**D**), *PEX11β* (**E**), *ABCD3* (**F**), *HSD17B4* (**G**), and *CAT* (**H**) ($n = 7$-16). **I–L**, Immunoblotting was performed on white matter from MS and non-MS controls ($n = 4$) targeting ASPA (**J**), PMP70 (**K**), and catalase (**L**), with representatives shown (**I**). β-actin was used as a control for protein loading. Error bars represent standard error of the mean. *$p < 0.05$; **$p < 0.01$; unpaired Student's *t* test. For primary antibodies used for Western blot, immunohistochemistry, and immunofluorescence, see Extended Data Figure 1-1. For PCR primer sequences used in this study, see Extended Data Figure 1-2.

The amount of time spent in the central section was defined as the "time in center." All animal experiments were performed according to the Canadian Council on Animal Care and local animal care and use committee guidelines.

PET imaging and analysis. PET imaging of 4-PBA- or solvent control-treated CPZ-exposed mice was performed 2 d before death, as described previously (Hamann et al., 2018). Mice were injected with translocator protein radioligand, [¹⁸F]DPA-714, via the tail vein to assess neuroinflammation. After an uptake period of 50 min, mice were anesthetized with isoflurane supplemented with oxygen, and static PET imaging was performed for 10 min using the Inveon PET scanner (Siemens Preclinical Solutions). The image was reconstructed using maximum *a posteriori* MAP reconstruction mode. Image files were further processed using the PMOD 4.004 imaging software Neuro tool (PMOD Technologies). Three-dimensional ROIs were selected for analysis with 50% thresholding. Mean standardized uptake value (mean = activity/ml tissue/injected activity/body weight, in ml/kg) was calculated for each ROI.

Statistical analyses. Comparisons between two groups were performed by unpaired Student's *t* test or by one-way ANOVA with appropriate *post hoc* test, using GraphPad Prism 8.0 (GraphPad Software).

Results

Peroxisome structural and biogenesis gene and protein expression is reduced in white matter of progressive MS patients

An earlier study reported that peroxisome protein expression was reduced in cortical neurons from people with MS (Gray et al., 2014). In the present studies, the expression of individual peroxisome genes was investigated in subcortical, normal-appearing white matter from patients with or without MS (Table 1). Analysis of the oligodendrocyte-enriched gene *ASPA* showed reduced transcript levels in the MS patient group (Fig. 1A). A gene expressed by CAMs, including resident
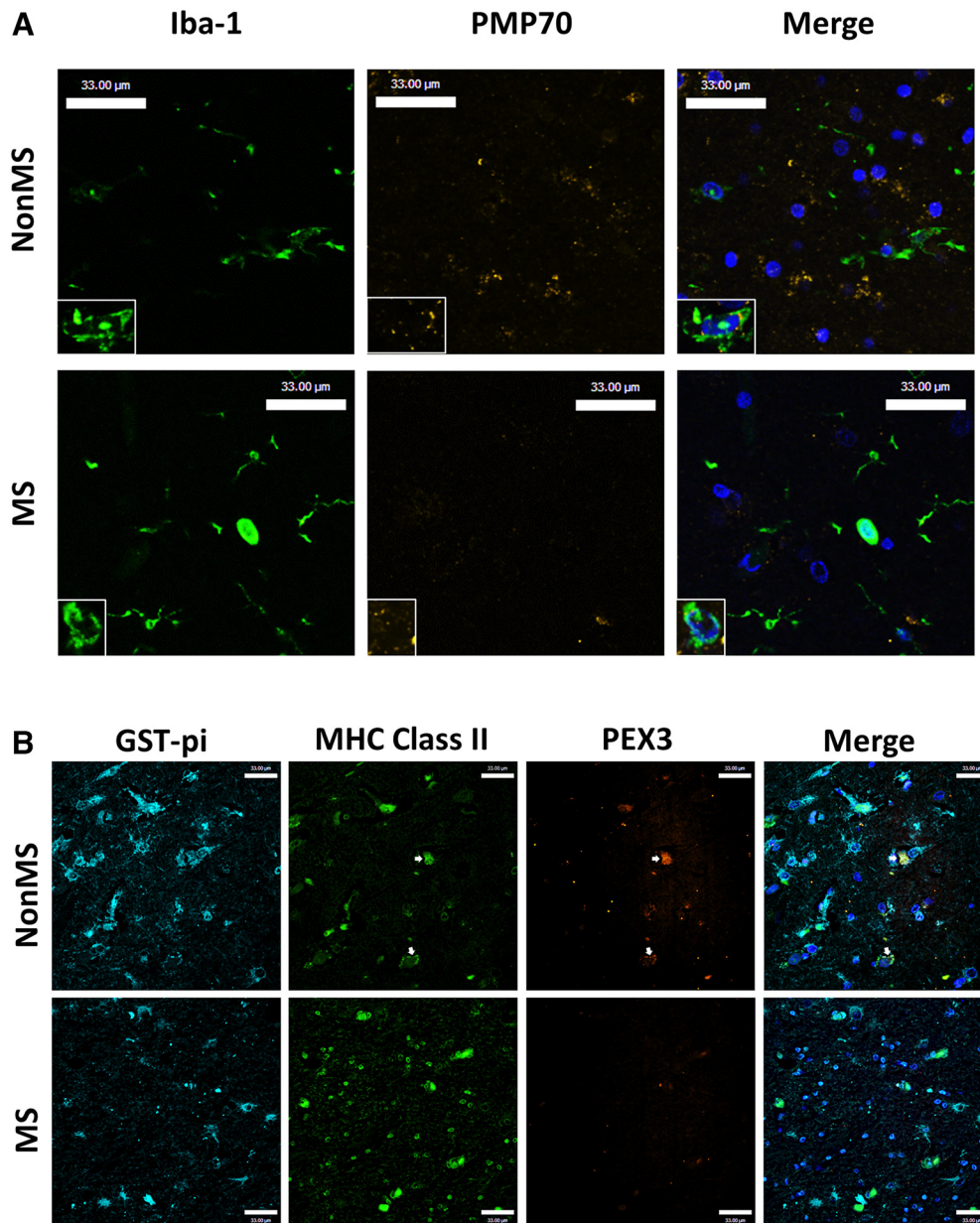
Figure 2. PMP70 and PEX3 immunoreactivity is suppressed in subcortical white matter of patients with MS. ***A***, Representative immunofluorescence images of white matter from MS patients and non-MS controls labeling Iba-1 (green), PMP70 (yellow), and DAPI (blue) with high-magnification inset. ***B***, Immunofluorescence image of subcortical white matter from a MS patient compared with a non-MS patient labeling GST-π (cyan), MHC II (green), PEX3 (orange), and DAPI (blue). Arrows point to MHC Class II positive cells with PEX3 immunostaining. Scale bars, 33 µm.

microglia and trafficking macrophages, *CD68*, showed increased expression in white matter for some patients in the MS group (Fig. 1*B*). Analysis of the peroxisome gene transcript levels revealed a consistent reduction in MS white matter, including *PEX3* (Fig. 1*C*), *PEX5L*, (Fig. 1*D*), and *HSD17B4* (Fig. 1*E*), although *ABCD3*, *PEX11β*, and catalase (*CAT*) (Fig. 1*F–H*) did not differ between groups. Immunoblotting showed that aspartoacylase (ASPA) and 70-kDa peroxisomal membrane protein (PMP70, encoded by *ABCD3*), but not catalase, protein levels (Fig. 1*I–L*) were reduced in white matter from MS patients compared with non-MS control patients. Immunofluorescence labeling of MS and non-MS frontal white matter with antibodies to ionized calcium-binding adaptor molecule 1 (Iba-1) to detect CAMs and peroxisomal marker PMP70 demonstrated that PMP70 immunoreactivity was decreased in the brains of MS patients, particularly in Iba-1-positive CAMs (Fig. 2*A*). Likewise, immunofluorescence

labeling with major histocompatibility complex class II (MHC II) to detect CAMs, the oligodendrocyte marker glutathione S-transferase pi (GST-π), and the peroxisomal membrane protein PEX3 showed that the majority of PEX3 immunolabeling was localized to CAMs and its immunoreactivity was decreased in the brains of the MS group (Fig. 2*B*). This observation was complemented by an expected reduction in GST-π immunoreactivity in MS tissues. Overall, these studies pointed to a reduction in peroxisome gene expression in white matter glia of the MS group, including CAMs and oligodendrocytes.

Inflammatory stimuli reduce peroxisome gene and protein expression in human microglia
To explore the comparative expression of individual peroxisome biogenesis and structural proteins in different neural cell types, immunoblotting was performed on lysates from
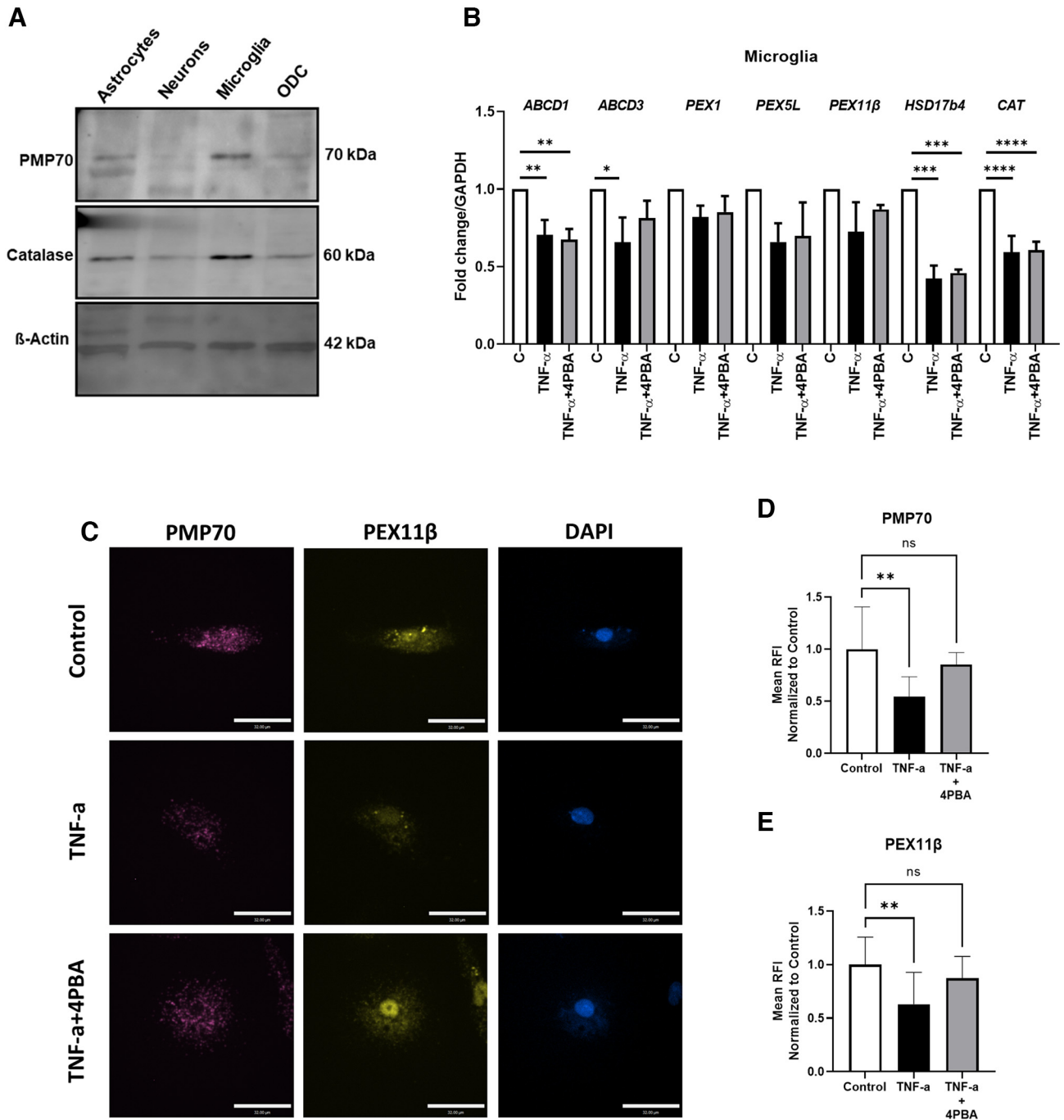
Figure 3. 4-PBA prevents decrease in peroxin protein levels, and *ABCD3* gene expression, by TNF-α in human microglia. **A**, Representative immunoblot showing PMP70 and catalase immunodetection in human fetal astrocytes, neurons, microglia, and oligodendrocyte (MO3.13) cell culture (ODC). **B–E**, Microglia were treated with TNF-α (50 ng/ml) for 24 h with or without 4-PBA (100 μM) or with vehicle control treatments. RNA was collected for RT-PCR analysis targeting *ABCD1*, *ABCD3*, *PEX1*, *PEX5L*, *PEX11β*, *HSD17b4*, and *CAT* (**B**) (n = 3 donors). Error bars represent standard error of the mean. Microglia were treated as above and fixed for immunofluorescence microscopy targeting PMP70 (magenta) and PEX11β (yellow). Representative images are shown (**C**) with quantification of mean fluorescence intensity of PMP70 (**D**) and PEX11β (**E**) (average of n = 10 cells for control, n = 8 cells for TNF-α, and n = 9 cells for TNF-α + 4-PBA). Error bars represent standard deviation. Scale bars, 32 μm. *$p < 0.05$; **$p < 0.005$; ***$p < 0.0005$; ****$p < 0.0001$; one-way ANOVA followed by Dunnett's *post hoc* test.

resting primary human neurons, microglia, astrocytes, and a human oligodendrocyte cell line (MO3.13) (Fig. 3A). Microglia displayed the highest levels of catalase and PMP70 protein relative to β-actin compared with the other cell types. These findings prompted investigation of the effects of a prototypic inflammatory stimulus, TNF-α, on the expression of peroxisome genes in primary human microglia, in the presence or absence of the peroxisome proliferator, 4-PBA. Exposure of primary microglia to TNF-α caused reduced transcript expression

of multiple peroxisome genes, including a significant reduction in *ABCD1*, *ABCD3*, *HSD17B4*, and *CAT* (Fig. 3B). Treatment of TNF-α-exposed cells with 4-PBA prevented a decrease in *ABCD3* expression. To verify these transcriptional changes, immunofluorescence labeling of microglia was performed (Fig. 3C), which revealed that PMP70 (Fig. 3D) and PEX11β (Fig. 3E) immunoreactivity levels were suppressed by TNF-α, as indicated by a significant reduction in relative mean fluorescence intensity. Treatment with 4-PBA prevented this decrease (Fig. 3D,E). Thus, peroxisome
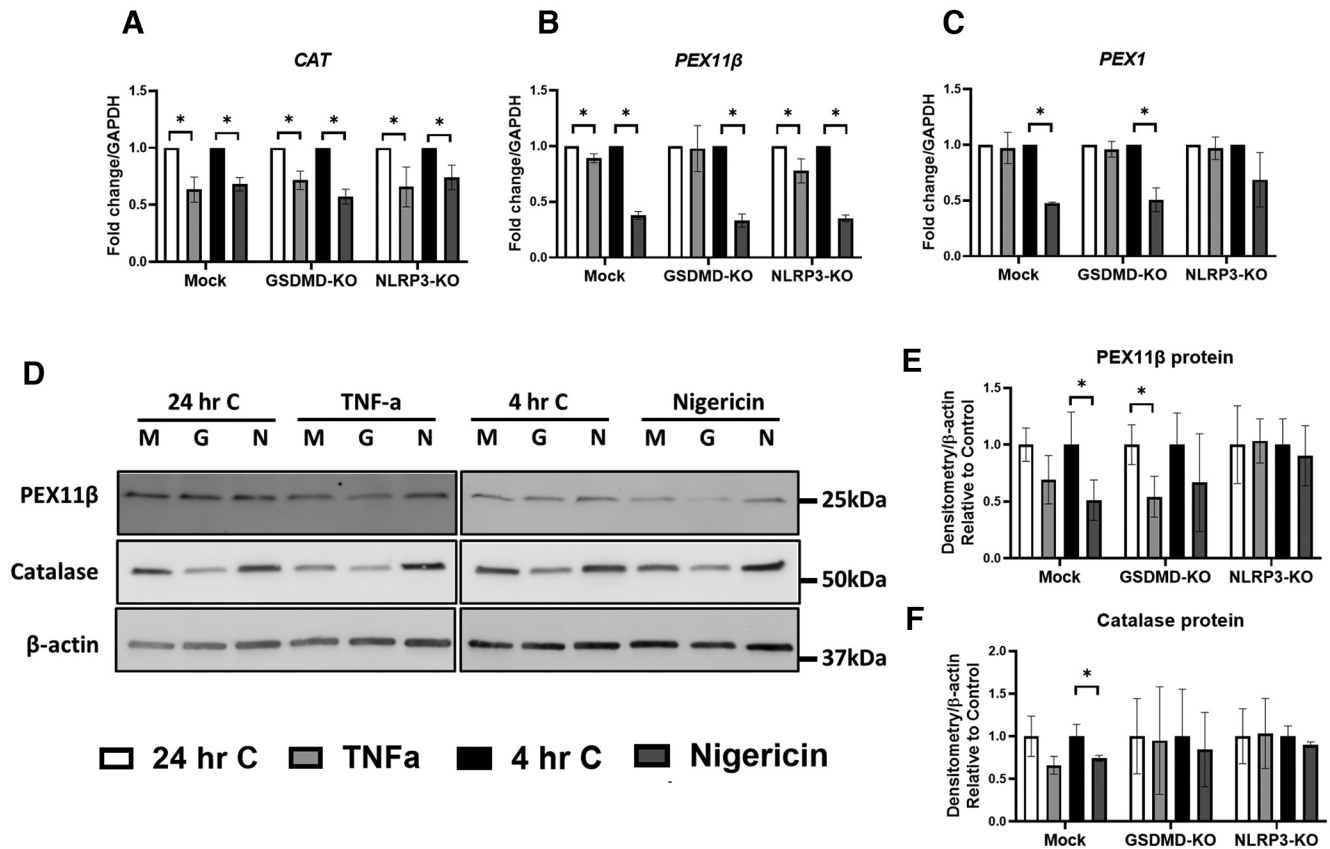
Figure 4. TNF-α and nigericin exposure reduces PEX11β protein in differentiated myeloid THP-1 cells in an NLRP3-dependent manner. *A–F*, Mock-deleted, GSDMD-KO, and NLRP3-KO THP-1 cells were differentiated with PMA for 18 h and treated with nigericin (6.7 μM) for 4 h or with TNF-α (50 ng/ml) for 24 h, together with an appropriate time-matched vehicle control. Following treatment, RNA was collected for RT-PCR analysis of peroxisome genes *CAT* (*A*), *PEX11β* (*B*), and *PEX1* (*C*), or cell lysates were collected for immunoblot analysis of peroxisomal proteins PEX11β and catalase (*D–F*). Quantification of immunoreactivity of PEX11β (*E*) and catalase (*F*) relative to that of a β-actin control for protein loading is shown normalized to time-matched vehicle control ($n = 3$-5). Error bars represent standard deviation. *$p < 0.05$ (unpaired Student's *t* test).

gene and protein expressions were sensitive to the effects of inflammation and *ABCD3* gene expression, and peroxisome protein was partially preserved by treatment with 4-PBA.

Peroxisome proteins are influenced by inflammasome activation

Both TNF-α and the bacterial molecule, nigericin, are known to induce inflammasome activation (McKenzie et al., 2018). Given the contribution of inflammasomes to neuroinflammation, including ROS production, the effects of inflammasome induction on the expression of peroxisome genes and proteins were examined in mock, GSDMD, or NLRP3 KO human macrophage-like (THP-1) cell lines (Fig. 4A–F). Gene editing was performed using CRISPR-Cas9 and verified as described (Platnich et al., 2018). Exposure of macrophage cells to TNF-α or nigericin showed that both stimuli suppressed *CAT* (Fig. 4A) and *PEX11β* (Fig. 4B) gene expression, whereas nigericin also suppressed *PEX1* (Fig. 4C) gene expression. KO of GSDMD prevented significant decrease of *PEX11β* expression in response to TNF-α (Fig. 4B), and NLRP3-KO prevented significant decrease in *PEX1* expression in response to nigericin (Fig. 4C). Gene expression of *ABCD3*, *ABCD1*, and *HSD17B4* were not as sensitive to the inflammatory stimuli, TNF-α or nigericin (data not shown). Immunoblot analyses (Fig. 4D) revealed that PEX11β protein levels were significantly decreased following exposure of GSDMD-KO cells to TNFα and were significantly reduced by nigericin in mock-deleted cells (Fig. 4E). PEX11β protein levels were

unchanged by TNF-α or nigericin in NLRP3-KO cells. Protein levels of catalase were not significantly affected by TNF-α but were significantly decreased by nigericin in mock-deleted cells (Fig. 4F). Nigericin exposure did not decrease catalase in either GSDMD-KO cells or NLRP3-KO cells. These data suggested that NLRP3 might modulate peroxisome protein expression in macrophage cells.

CPZ-induced demyelination results in induction of inflammasome genes and suppression of peroxisome gene and protein expression

CPZ is a recognized mediator of brain demyelination, likely through its capacity to chelate copper, that results in mitochondrial injury (Vega-Riquer et al., 2019). Transcriptional time course studies of cerebellum in susceptible mice disclosed that oligodendrocyte marker gene *Aspa* and peroxisomal genes *Pex3*, *Pex11β*, *Hsd17b7*, and *Abcd1* were suppressed after 4 weeks of CPZ exposure but returned to baseline at 6 weeks (data not shown). These findings prompted design of experiments in which CPZ was provided to animals for 4 weeks with initiation of 4-PBA therapy 2 weeks after initiation of CPZ (Fig. 5A). In the hindbrain of animals (cerebellum and brainstem), CPZ exposure resulted in suppression of *Aspa* gene expression in both control and 4-PBA-treated animals compared with unexposed animals (Fig. 5B). Moreover, CPZ exposure induced the inflammasome genes *Asc* (Fig. 5C), *Nlrp3* (Fig. 5D), and *Il-1β* (Fig. 5E) compared with unexposed animals. 4-PBA treatment prevented the increase in *Il-1β* and *Nlrp3* expression, but not the
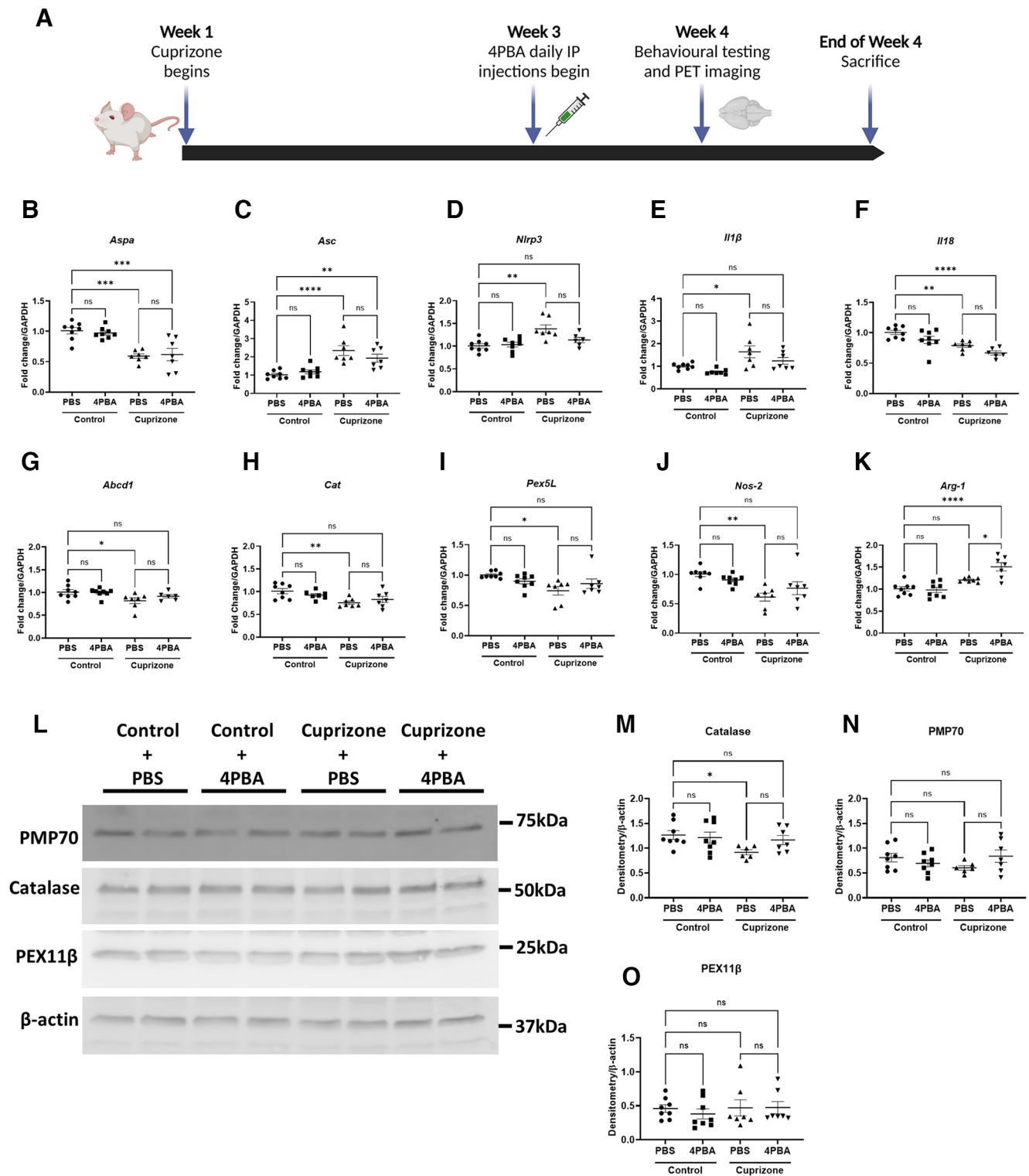
Figure 5. CPZ exposure in mice decreases expression of peroxisome biogenesis and structural genes and increases inflammasome gene expression in the hindbrain. Mice were fed control chow or chow containing 0.265% CPZ for 4 weeks and treated with PBS or 4-PBA (100 mg/kg) intraperitoneally during weeks 3 and 4 of CPZ exposure. Behavioral testing and PET imaging were performed before death at the end of week 4. **A**, Schematic diagram of mouse treatment regimen created with www.BioRender.com. **B–K**, Hindbrains of mice (including brainstem and cerebellum) were analyzed by RT-PCR targeting peroxisome and inflammatory genes *Aspa* (**B**), *Asc* (**C**), *Nlrp3* (**D**), *Il1β* (**E**), *Il18* (**F**), *Abcd1* (**G**), *Cat* (**H**), *Pex5l* (**I**), *Nos-2* (**J**), and *Arg-1* (**K**) ($n = 6$-8). Error bars represent standard error of the mean. $*p < 0.05$; $**p < 0.005$; $***p < 0.0005$; $****p < 0.0001$; one-way ANOVA with Tukey's *post hoc* test. **L–O**, Immunoblotting and quantification of peroxisomal proteins catalase (**M**), PMP70 (**N**), and PEX11β (**O**), with representative immunoblot shown (**L**) ($n = 6$-8). Error bars represent standard error of the mean. $*p < 0.05$ (one-way ANOVA with Welch's correction followed by Dunnett's T3 *post hoc* test).

increased expression of *Asc* (Fig. 5C–E). In contrast, *Il-18* transcript levels were suppressed in both CPZ-exposed groups (Fig. 5F). CPZ also caused significant suppression in peroxisome transcripts *Abcd1* (Fig. 5G), *Cat* (Fig. 5H), and *Pex5l* (Fig. 5I), which was prevented by

4-PBA treatment. Of note, *Nos-2* expression was diminished by CPZ exposure (Fig. 5J), while *Arg-1* expression was induced by 4-PBA treatment of CPZ-exposed animals (Fig. 5K), suggesting that 4-PBA treatment promoted a neuroprotective CAM phenotype.
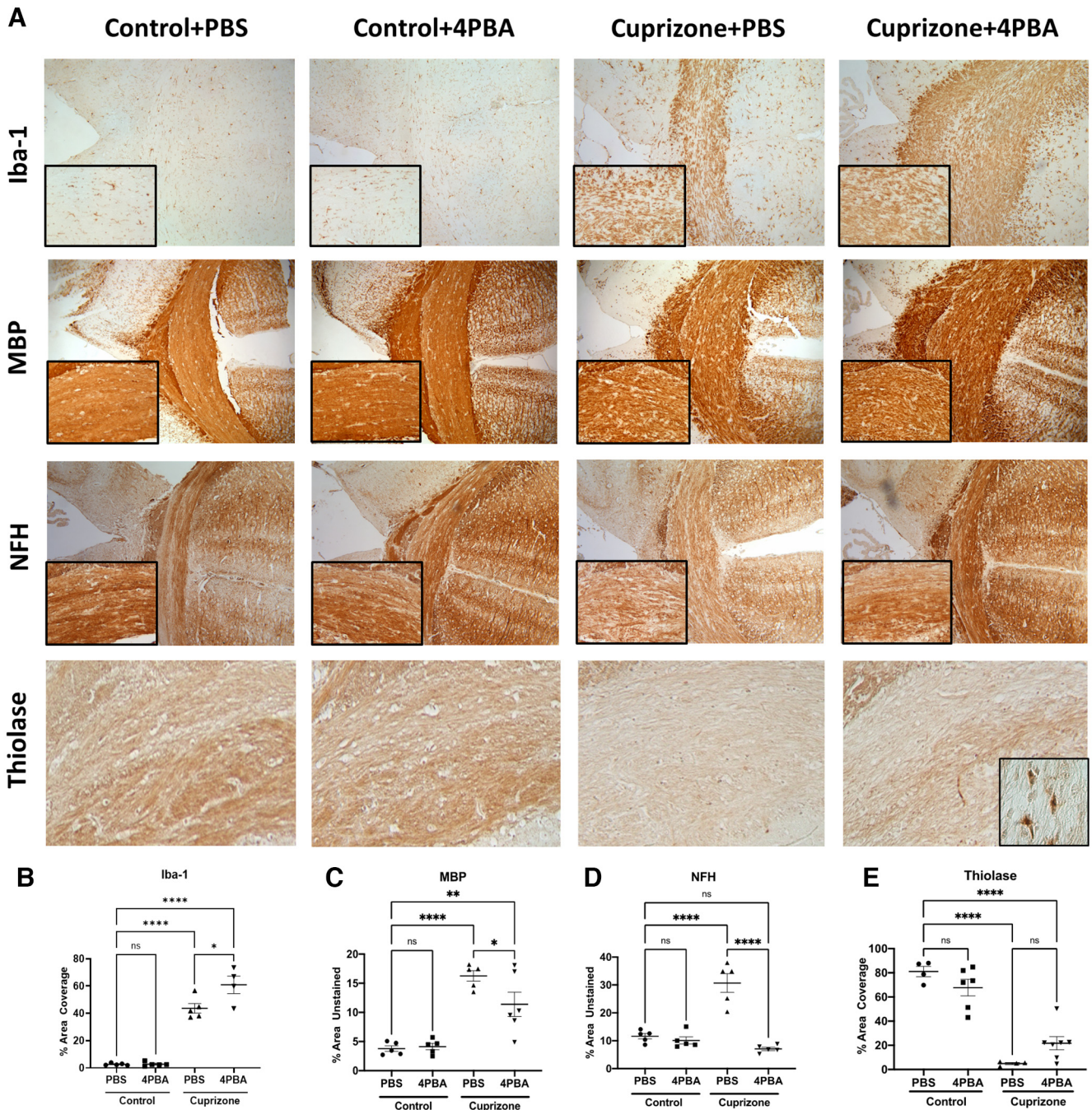
Figure 6. CPZ exposure causes demyelination and axonal injury, while 4-PBA treatment is associated with enhanced CAM recruitment and preserved myelin, axonal, and peroxisomal structure. *A–E,* Immunohistochemistry of mouse central corpus callosum following CPZ exposure (0.265%) with or without 4-PBA treatment. Representative images (10×) with high-magnification inset (20×) (*A*) and quantification of Iba-1% area coverage (*B*), MBP percent unstained area (*C*), NFH percent unstained area (*D*), and thiolase percent area coverage (*E*) of the central corpus callosum. Error bars represent standard error of the mean. *$p < 0.05$; **$p < 0.005$; ***$p < 0.0005$; ****$p < 0.0001$; one-way ANOVA followed by Tukey's *post hoc* test.

Immunoblotting of brain lysates revealed that catalase protein was reduced in CPZ-exposed animals, although 4-PBA prevented this reduction (Fig. 5*M*). Protein levels of PMP70 or PEX11β were similar for all four groups (Fig. 5*N,O*). Our results suggested that CPZ exposure suppressed the expression of several peroxisome genes, but 4-PBA partially prevented this suppression.

4-PBA treatment prevents CPZ-mediated CAM activation, demyelination, axonal loss, and peroxisome loss

The effects of CPZ exposure were also apparent from morphologic analyses of the central corpus callosum. Immunolabeling of

the CAM marker, Iba-1 (Fig. 6*A*), showed increased immuno-positive cells (%) in the CPZ-exposed animals compared with control, which was further increased by 4-PBA treatment (Fig. 6*B*). Quantification of myelin structure using MBP immunoreactivity revealed that CPZ exposure reduced immunolabeling in the central corpus callosum compared with controls, as indicated by a relative increase (%) in unlabeled tissue, which was reversed by 4-PBA (Fig. 6*C*). Similarly, quantification of axonal integrity measured by using neurofilament H (NFH) immunoreactivity revealed that CPZ significantly increased the area of tissue that was not immunolabeled for NFH, although this effect
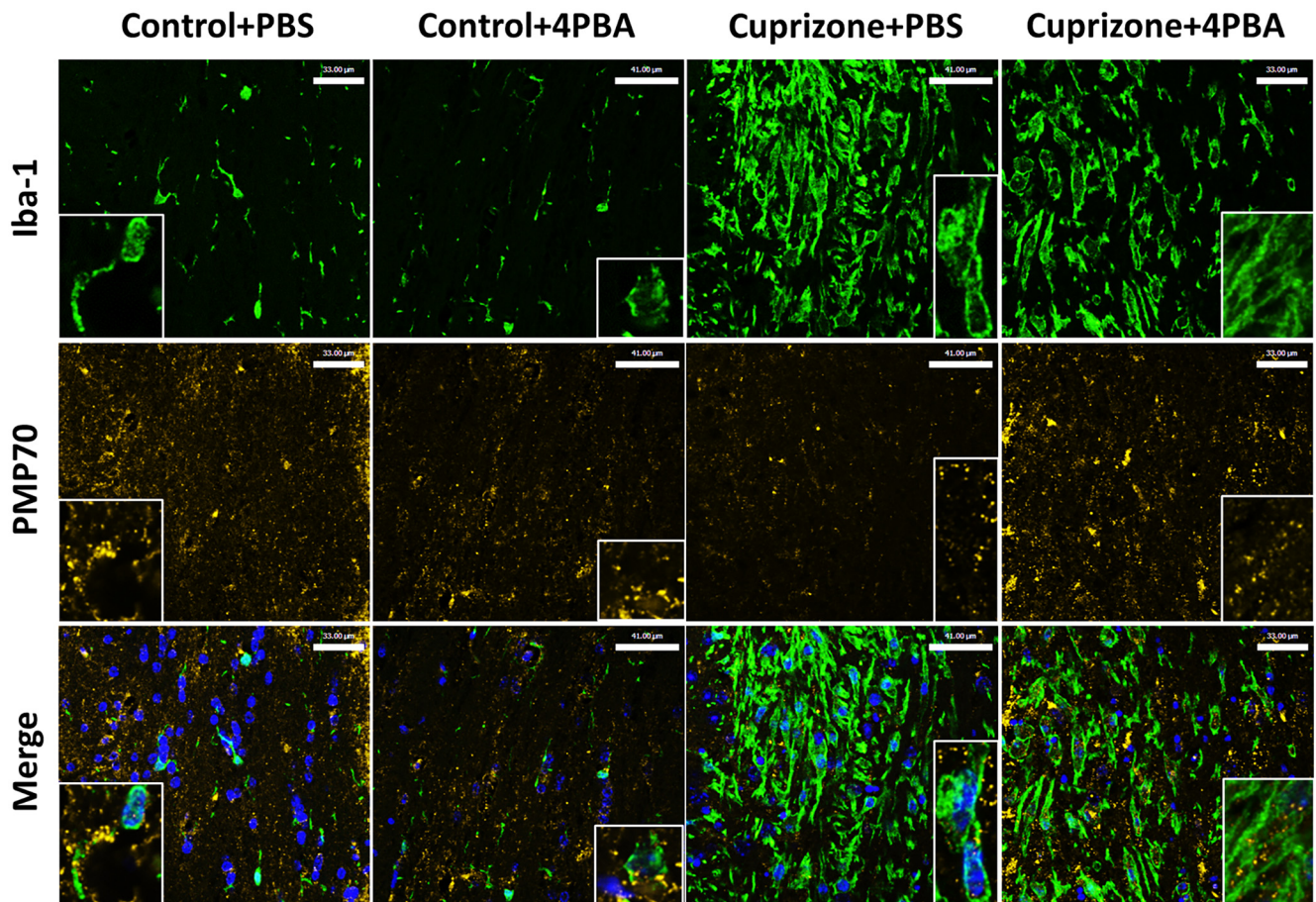
Figure 7. CPZ suppresses PMP70 immunostaining, particularly in Iba-1-positive cells, which is restored by 4-PBA treatment. Representative immunofluorescence image of central corpus callosum of mice following CPZ exposure (0.265%) with or without 4-PBA treatment labeling Iba-1 (green), PMP70 (yellow), and DAPI (blue) with high-magnification (40×) insets. Scale bars: control + PBS and CPZ + 4-PBA, 33 μm; Control + 4PBA and CPZ + PBS, 41 μm.

was prevented by 4-PBA treatment (Fig. 6D). Analysis of the peroxisomal thiolase immunoreactivity in the central corpus callosum was reduced by CPZ exposure, although 4-PBA treatment partially restored thiolase expression (Fig. 6E), especially in glial cells within the corpus callosum (Fig. 6E, inset). These data implied that, while CPZ induced innate immune activation with associated myelin and neuro-axonal injury, 4-PBA's effects were neuroprotective in this model evident as preserved myelin and axonal structural integrity.

We performed immunofluorescence microscopy in the four experimental groups, labeling for CAM marker Iba-1 and peroxisome marker PMP70 to assess whether CPZ-mediated peroxisomal dysfunction in CAM is mitigated by 4-PBA treatment (Fig. 7). CPZ caused pronounced increase in Iba-1 staining, which remained elevated with 4-PBA treatment, similar to our immunohistochemistry results. CPZ appeared to reduce PMP70 immunostaining, particularly in Iba-1-immunopositive cells, which was prevented with 4-PBA treatment.

PET imaging and neurobehavioral effects of CPZ-exposed and unexposed animals
To define further the effects of CPZ exposure, PET imaging of the translocator protein (TSPO)-binding radioligand, [18F]DPA-714, was performed to assess CAM activation and function (Zinnhardt et al., 2019). TSPO is primarily expressed on activated CAMs, although it is also expressed on astrocytes, neural stem cells, and vascular endothelial cells (Betlazar et al., 2020,

2021; Van Camp et al., 2021). Increased TSPO PET imaging is a surrogate for neuroinflammation. We assessed whole-brain uptake of [18F]DPA-714 in the four experimental conditions (Fig. 8A–D). There was a trend for CPZ to increase [18F]DPA-714 uptake, which was normalized by 4-PBA (Fig. 8E). These findings suggested that CPZ activated CAMs, as reflected by increased [18F]DPA-714 ligand binding, which was prevented with 4-PBA. We also evaluated the effects of CPZ and 4-PBA treatments on neurobehavior performance. There was no difference in time spent in the center of an open field for all treatments (Fig. 8F). Conversely, CPZ exposure reduced the number of crossings of the open field, which was restored by 4-PBA treatment (Fig. 8G). Rearing was also reduced in CPZ-exposed animals and restored by 4-PBA treatment (Fig. 8H). These studies indicated that specific neurobehavioral tasks were impaired by CPZ exposure, although they could be restored by treatment with 4-PBA.

Discussion
In this study, disrupted peroxisome gene expression and its sequelae were examined using a multiplatform approach, including autopsied patient brain tissues, primary and KO human myeloid cells, and a CPZ mouse model. Our studies showed that peroxisome gene and protein expression were suppressed in cerebral white matter from MS patients compared with non-MS controls. An MS-relevant stimulus, TNF-α, suppressed peroxisome
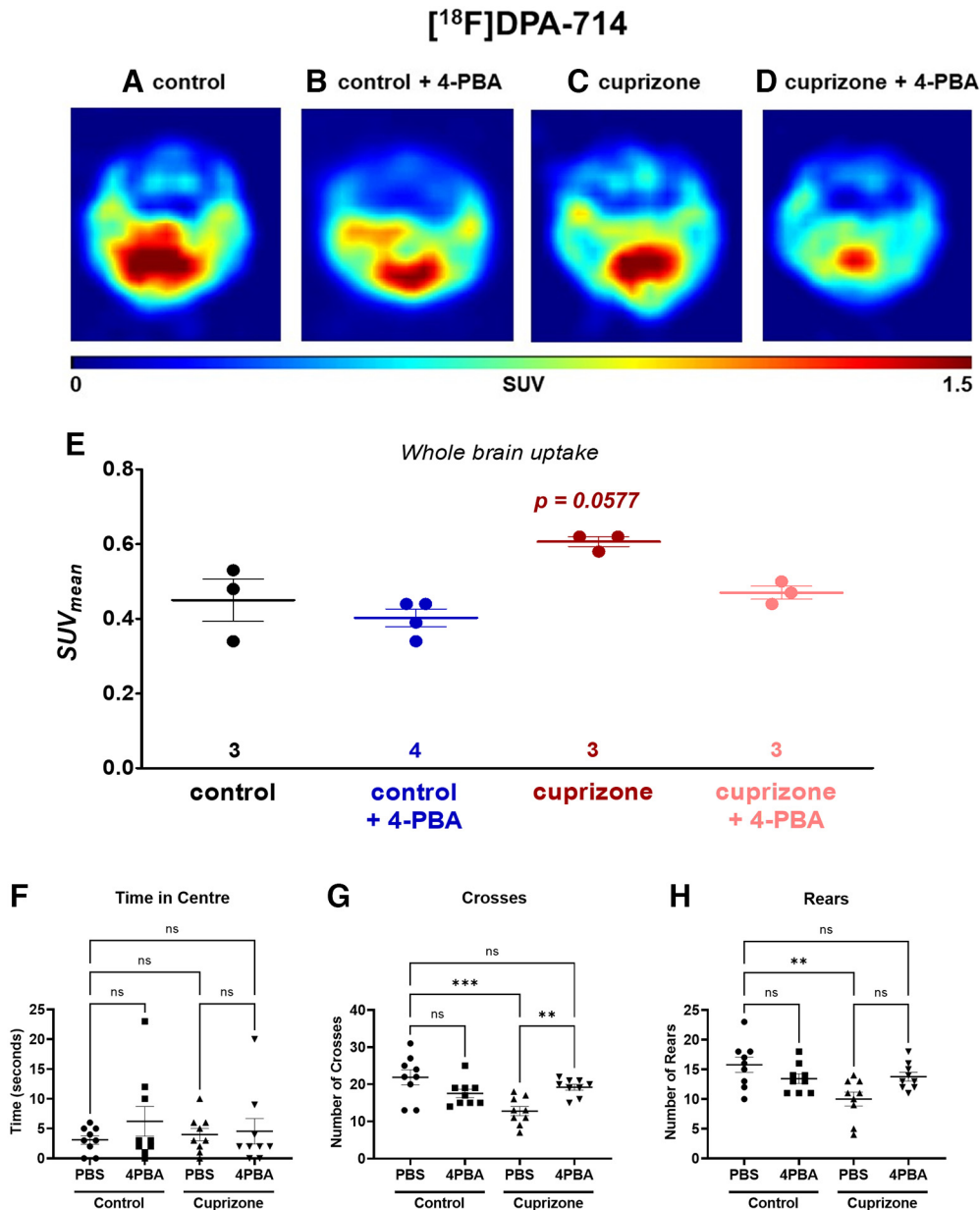
Figure 8. 4-PBA treatment ameliorated neuroinflammation by PET imaging and improved neurobehavioral outcomes in CPZ-exposed animals. ***A–E***, PET imaging of neuroinflammation and CAM activation by CPZ-induced demyelination in mouse brain using [^{18}F]DPA-18. Representative axial images under (***A***) control, (***B***) 4-PBA therapy, (***C***) CPZ administration, and (***D***) 4-PBA therapy in CPZ-treated mice. ***E***, Semiquantitative standardized uptake value (SUV$_{mean}$) values for the whole-brain uptake as mean $\pm$ SEM values from *n* mice. *$p < 0.05$ (one-way ANOVA followed by Tukey's *post hoc* test). ***F, G***, Open field locomotor test was performed on mice at the beginning of week 4, and the time spent in the center (***F***), the number of crosses (***G***), and the number of rears (***H***) were assessed over a 5 min period and quantified. *$p < 0.05$; **$p < 0.005$; ***$p < 0.0005$; one-way ANOVA, followed by Sidak's select comparisons *post hoc* test.

gene and protein expression in microglia, and the latter was partially prevented by the peroxisome proliferator, 4-PBA (Sexton et al., 2010). KO of inflammasome genes in a macrophage cell line, THP-1, revealed that suppression of PEX11β and catalase by inflammatory stimuli was dependent on NLRP3 expression. In mice, CPZ exposure suppressed peroxisome gene expression and induced inflammasome genes in the brain. CPZ exposure also caused demyelination, axonal injury, and increased CAM reactivity in the central corpus callosum. While 4-PBA treatment preserved peroxisome gene expression and limited inflammasome gene expression, it concurrently promoted CAM induction with associated induction of the *Arg-1* gene, suggesting that 4-PBA might direct CAMs toward a neuroprotective phenotype. PET imaging showed that 4-PBA treatment prevented an increase in

TSPO radioligand binding caused by CPZ exposure. This finding was complemented by 4-PBA-mediated improvements in neurobehavioral outcomes in CPZ-exposed animals. To our knowledge, this is the first study to show the following: (1) peroxisome genes and protein levels were suppressed in white matter of MS patients and CPZ-exposed mice, (2) MS-relevant inflammatory stimuli caused peroxisome dysfunction in CAMs, (3) suppression of peroxisome gene expression was modulated by the NLRP3 inflammasome, and (4) 4-PBA treatment preserved peroxisome function in CAMs, resulting in improved neurobehavioral, molecular, and morphologic outcomes.

Decreased PMP70 (encoded by *ABCD3*) immunoreactivity as well as *ABCD3* mRNA expression, along with increased hexacosanoic acid (C26:0) levels, have been reported in gray matter of

patients with MS (Gray et al., 2014). Peroxisome function was impaired in brain in a rat model of experimental autoimmune encephalomyelitis, as reflected by accumulation of hexacosanoic acid (C26:0), depletion of plasmalogens, and impaired activity of the peroxisomal enzymes catalase and dihydroxyacetonephosphate acyltransferase (Singh et al., 2004). In line with these observations, we observed decreased levels of critical peroxisome biogenesis and structural genes in the white matter of MS patients, along with decreased PMP70 protein levels and decreased PMP70 and PEX3 immunoreactivity. PMP70 is an ATPase present on peroxisome membranes, which actively transports very-long chain fatty acids into the peroxisome for β-oxidation. Mutations in PMP70 are responsible for some forms of Zellweger's syndrome (Gärtner et al., 1992), which is associated with severe neurologic symptoms (Weller et al., 2003). PEX3 is critical for both insertion of peroxisome membrane proteins into the peroxisome membrane and for *de novo* peroxisome biogenesis, and KO of PEX3 in human fibroblasts results in complete ablation of peroxisomes (Jean Beltran et al., 2018; Farré et al., 2019). Deficits in peroxins may contribute to the observed decrease in *ASPA* (oligodendrocyte marker) expression, and oligodendrocyte ASPA immunoreactivity in white matter of human patients (Fig. 1), as oligodendrocytes rely on peroxisomes for both ROS homeostasis and myelin synthesis (Kassmann, 2014; Berger et al., 2016).

Microglia serve an important role in the pathogenesis of MS by promoting inflammation in demyelinating lesions, as well as by contributing to remyelination (Guerrero and Sicotte, 2020). Although the contributions of peroxisomes to oligodendrocyte function are well documented (Kassmann, 2014), we focused on CAMs because of the comparative abundance of peroxisomal proteins in microglia versus other brain cell types (Fig. 3A). In microglia, peroxisomes modulate antiviral Type I interferon responses, and previous studies from our laboratory reported reduced expression of peroxisome biogenesis and structural genes in pegivirus-infected microglia (Doan et al., 2021). Exposing human fetal microglia to TNF-α decreased expression of peroxisome transcripts as well as PEX11β and PMP70 immunoreactivity. PEX11β is critical for maintaining peroxisome abundance, as it is responsible for elongating peroxisomes in the growth and division model of peroxisome biogenesis. *ABCD3* (which encodes PMP70) gene expression and PEX11β and PMP70 immunoreactivity were partially preserved by the peroxisome proliferator, 4-PBA. In CPZ-exposed mice, 4-PBA treatment also restored peroxisome gene and protein expression in the hindbrain, prevented demyelination and axonal injury in the corpus callosum, and improved neurobehavioral outcomes. The increase in Iba-1 immunostaining in the corpus callosum, along with the induction of *Arg-1* gene expression, suggested that 4-PBA might promote a neuroprotective CAM phenotype (Cherry et al., 2014). 4-PBA exerts other actions apart from its binding and activation of peroxisome proliferator-activated receptors (Liu et al., 2002), including acting as a histone deacetylase inhibitor (Kusaczuk et al., 2015) and as a chemical chaperone (Ozcan et al., 2006). Indeed, 4-PBA is used as a treatment for urea cycle disorders (Kolb et al., 2015). However, our preliminary studies using data from a drug library screen suggested that 4-PBA is also an effective promoter of peroxisome functions, especially in myeloid cells (Di Cara et al., 2017; Liu et al., 2021). Indeed, 4-PBA is known to have anti-inflammatory effects in leukocytes (Geng et al., 2019) and appears to reduce disease severity and endoplasmic reticulum stress in experimental autoimmune encephalomyelitis models

(Dasgupta et al., 2003; Yousuf et al., 2020). 4-PBA is well tolerated and is apparently neuroprotective in clinical trials (Paganoni et al., 2021), making it a potential therapy for MS.

Previous studies have shown peroxisomes can indirectly regulate the NLRP3 inflammasome through the actions of the peroxisome-localized protein, c13orf31 (FAMIN) (Cader et al., 2016). KO of FAMIN in murine macrophages resulted in lower levels of active IL-1β (P17) and caspase-1 (P20) proteins in response to LPS and ATP. Of note, more recent studies have localized FAMIN to the cytosol and nucleus, but not peroxisomes, in mouse macrophages (Skon-Hegg et al., 2019). To the best of our knowledge, our study is the first to demonstrate that NLRP3 regulates peroxisome protein expression. KO of NLRP3 preserved both PEX11β and catalase protein levels in THP-1 cells exposed to inflammatory stimuli. Although catalase protein was also preserved by GSDMD KO, the basal levels of catalase appeared to be lower in the GSDMD-KO cell line versus mock- or NLRP3 KO cells. We also showed that reduction in peroxisome genes and proteins by CPZ exposure was associated with an increase in *Nlrp3* and *Il1β* gene expression (Fig. 5D,E). Treatment with 4-PBA partially preserved peroxisome gene expression and protein levels and prevented an increase in *Nlrp3* expression. As we did not directly measure inflammasome activation in the present CPZ experiments, future studies could determine whether improving peroxisome integrity with 4-PBA affects inflammasome activation in CPZ-exposed mice. Future studies are also needed to identify whether the actions of NLRP3 on regulating peroxisome protein levels are mediated via inflammasome activation or through other mechanisms.

The present study faced several challenges. For example, the autopsy cohort was limited to patients with chronic MS and other disease controls. This selection could have biased observations by underestimating the magnitude of differences in peroxisome gene expression and protein levels between MS and non-MS subjects because other disease control (non-MS) subjects might also have had peroxisomal injury. The use of human fetal microglia for the present *in vitro* studies could also have affected the differences between groups compared with the use of adult microglia or monocyte-derived macrophages. Although fetal microglia differ from adult in several ways, they are largely unaffected by donor comorbidities (e.g., drug exposure and trauma), which can be a confounder in adult tissue and cells. In the present studies, we have used Iba-1 immunolabeling to identify CAMs in brain tissue as Iba-1 is a validated marker of neuroinflammation in MS (Walker and Lue, 2015). However, Iba-1 is not specific to resident microglia as it also stains blood-derived macrophages (Imai et al., 1996). Therefore, future studies are needed to investigate the relative contributions of peroxisome injury in resident microglia versus blood-derived macrophages during MS. The CPZ model does not fully recapitulate progressive MS in that there is limited macrophage infiltration into the brain, and lymphocytes do not participate in the model's pathogenesis unlike in progressive MS. In order to reduce the number of animals used herein, we investigated (1) the hindbrain (cerebellum and brainstem) for molecular analysis and (2) the forebrain (central corpus callosum) for immunohistochemical and immunofluorescence imaging. Regional differences in peroxisome gene and protein expression in both health and disease may exist between different anatomic brain locations, although the CPZ model causes demyelination to the cerebellum in a similar fashion to the corpus callosum (Ludwin, 1978; Skripuletz et al., 2010). In our CPZ mouse model, we performed PET analysis using TSPO ligand. Although TSPO is expressed on activated

CAMs, it is also expressed to some degree in vascular endothelial cells, neural stem cells, and activated astrocytes (Betlazar et al., 2020, 2021; Van Camp et al., 2021). Thus, each experimental platform has limitations that are to some extent overcome by the consistency of the current findings across all approaches. Finally, the protective effects of 4-PBA on the brain may be due, in part, to its mitigating effects on ER stress in addition to its peroxisome proliferating properties.

Biomarkers and treatments for MS remain an overarching need in the clinical care of patients with MS. The present observations point to new insights into the pathogenesis of MS that encompasses novel pathways that remain to be explored fully in terms of potential biomarkers for diagnosis and disease course as well as responses to therapy. Moreover, therapeutic targeting of peroxisome-associated pathways might be a potentially valuable strategy for treating MS and other neuroinflammatory diseases.

References

Barclay W, Shinohara ML (2017) Inflammasome activation in multiple sclerosis and experimental autoimmune encephalomyelitis (EAE). Brain Pathol 27:213–219.

Berger J, Dorninger F, Forss-Petter S, Kunze M (2016) Peroxisomes in brain development and function. Biochim Biophys Acta 1863:934–955.

Betlazar C, Middleton RJ, Banati R, Liu GJ (2020) The translocator protein (TSPO) in mitochondrial bioenergetics and immune processes. Cells 9:512.

Betlazar C, Middleton RJ, Howell N, Storer B, Davis E, Davies J, Banati R, Liu GJ (2021) Mitochondrial translocator protein (TSPO) expression in the brain after whole body gamma irradiation. Front Cell Dev Biol 9:715444.

Boghozian R, McKenzie BA, Saito LB, Mehta N, Branton WG, Lu J, Baker GB, Noorbakhsh F, Power C (2017) Suppressed oligodendrocyte steroidogenesis in multiple sclerosis: implications for regulation of neuroinflammation. Glia 65:1590–1606.

Cader MZ, et al. (2016) C13orf31 (FAMIN) is a central regulator of immunometabolic function. Nat Immunol 17:1046–1056.

Cherry JD, Olschowka JA, O'Banion MK (2014) Neuroinflammation and M2 microglia: the good, the bad, and the inflamed. J Neuroinflammation 11:98.

Coll RC, et al. (2015) A small-molecule inhibitor of the NLRP3 inflammasome for the treatment of inflammatory diseases. Nat Med 21:248–255.

Dasgupta S, Zhou Y, Jana M, Banik NL, Pahan K (2003) Sodium phenylacetate inhibits adoptive transfer of experimental allergic encephalomyelitis in SJL/J mice at multiple steps. J Immunol 170:3874–3882.

Di Cara F, Sheshachalam A, Braverman NE, Rachubinski RA, Simmonds AJ (2017) Peroxisome-mediated metabolism is required for immune response to microbial infection. Immunity 47:93–106.e107.

Di Cara F, Andreoletti P, Trompier D, Vejux A, Bulow MH, Sellin J, Lizard G, Cherkaoui-Malki M, Savary S (2019) Peroxisomes in immune response and inflammation. Int J Mol Sci 20:3877.

Dixit E, Boulant S, Zhang Y, Lee AS, Odendall C, Shum B, Hacohen N, Chen ZJ, Whelan SP, Fransen M, Nibert ML, Superti-Furga G, Kagan JC (2010) Peroxisomes are signaling platforms for antiviral innate immunity. Cell 141:668–681.

Doan MA, Roczkowsky A, Smith M, Blevins G, van Landeghem FK, Gelman BB, Branton WG, Stapleton JT, Hobman TC, Power C (2021) Infection of glia by human pegivirus suppresses peroxisomal and antiviral signaling pathways. J Virol 95:0107421.

Farré JC, Mahalingam SS, Proietto M, Subramani S (2019) Peroxisome biogenesis, membrane contact sites, and quality control. EMBO Rep 20: e46864.

Filippi M, Bar-Or A, Piehl F, Preziosa P, Solari A, Vukusic S, Rocca MA (2018) Multiple sclerosis. Nat Rev Dis Primers 4:43.

Gärtner J, Moser H, Valle D (1992) Mutations in the 70K peroxisomal membrane protein gene in Zellweger syndrome. Nat Genet 1:16–23.

Geng S, Zhang Y, Lee C, Li L (2019) Novel reprogramming of neutrophils modulates inflammation resolution during atherosclerosis. Sci Adv 5: eaav2309.

Gray E, Rice C, Hares K, Redondo J, Kemp K, Williams M, Brown A, Scolding N, Wilkins A (2014) Reductions in neuronal peroxisomes in multiple sclerosis grey matter. Mult Scler 20:651–659.

Guerrero BL, Sicotte NL (2020) Microglia in multiple sclerosis: friend or foe? Front Immunol 11:374.

Hamann I, Krys D, Glubrecht D, Bouvet V, Marshall A, Vos L, Mackey JR, Wuest M, Wuest F (2018) Expression and function of hexose transporters GLUT1, GLUT2, and GLUT5 in breast cancer: effects of hypoxia. FASEB J 32:5104–5118.

Hemmer B, Kerschensteiner M, Korn T (2015) Role of the innate and adaptive immune responses in the course of multiple sclerosis. Lancet Neurol 14:406–419.

Hjorth E, Freund-Levi Y (2012) Immunomodulation of microglia by docosahexaenoic acid and eicosapentaenoic acid. Curr Opin Clin Nutr Metab Care 15:134–143.

Hulshagen L, Krysko O, Bottelbergs A, Huyghe S, Klein R, Van Veldhoven PP, De Deyn PP, D'Hooge R, Hartmann D, Baes M (2008) Absence of functional peroxisomes from mouse CNS causes dysmyelination and axon degeneration. J Neurosci 28:4015–4027.

Imai Y, Ibata I, Ito D, Ohsawa K, Kohsaka S (1996) A novel gene iba1 in the major histocompatibility complex class III region encoding an EF hand protein expressed in a monocytic lineage. Biochem Biophys Res Commun 224:855–862.

Jaudszus A, Gruen M, Watzl B, Ness C, Roth A, Lochner A, Barz D, Gabriel H, Rothe M, Jahreis G (2013) Evaluation of suppressive and pro-resolving effects of EPA and DHA in human primary monocytes and T-helper cells. J Lipid Res 54:923–935.

Jean Beltran PM, Cook KC, Hashimoto Y, Galitzine C, Murray LA, Vitek O, Cristea IM (2018) Infection-induced peroxisome biogenesis is a metabolic strategy for herpesvirus replication. Cell Host Microbe 24:526–541. e527.

Kassmann CM (2014) Myelin peroxisomes: essential organelles for the maintenance of white matter in the nervous system. Biochimie 98:111–118.

Kolb PS, Ayaub EA, Zhou W, Yum V, Dickhout JG, Ask K (2015) The therapeutic effects of 4-phenylbutyric acid in maintaining proteostasis. Int J Biochem Cell Biol 61:45–52.

Kusaczuk M, Bartoszewicz M, Cechowska-Pasko M (2015) Phenylbutyric acid: simple structure - multiple effects. Curr Pharm Des 21:2147–2166.

Liu N, Qiang W, Kuang X, Thuillier P, Lynn WS, Wong PK (2002) The peroxisome proliferator phenylbutyric acid (PBA) protects astrocytes from ts1 MoMuLV-induced oxidative cell death. J Neurovirol 8:318–325.

Liu Y, Weaver CM, Sen Y, Eitzen G, Simmonds AJ, Linchieh L, Lurette O, Hebert-Chatelain E, Rachubinski RA, Di Cara F (2021) The nitric oxide donor, S-nitrosoglutathione, rescues peroxisome number and activity defects in PEX1G843D mild Zellweger syndrome fibroblasts. Front Cell Dev Biol 9:714710.

Ludwin SK (1978) Central nervous system demyelination and remyelination in the mouse: an ultrastructural study of cuprizone toxicity. Lab Invest 39:597–612.

Maingat FG, Polyak MJ, Paul AM, Vivithanaporn P, Noorbakhsh F, Ahboucha S, Baker GB, Pearson K, Power C (2013) Neurosteroid-mediated regulation of brain innate immunity in HIV/AIDS: DHEA-S suppresses neurovirulence. FASEB J 27:725–737.

Malhotra S, et al. (2020) NLRP3 inflammasome as prognostic factor and therapeutic target in primary progressive multiple sclerosis patients. Brain 143:1414–1430.

Mamik MK, Hui E, Branton WG, McKenzie BA, Chisholm J, Cohen EA, Power C (2017) HIV-1 viral protein R activates NLRP3 inflammasome in microglia: implications for HIV-1 associated neuroinflammation. J Neuroimmune Pharmacol 12:233–248.

Mamik MK, Asahchop EL, Chan WF, Zhu Y, Branton WG, McKenzie BA, Cohen EA, Power C (2016) Insulin treatment prevents neuroinflammation and neuronal injury with restored neurobehavioral function in models of HIV/AIDS neurodegeneration. J Neurosci 36:10683–10695.

McKenzie BA, Mamik MK, Saito LB, Boghozian R, Monaco MC, Major EO, Lu JQ, Branton WG, Power C (2018) Caspase-1 inhibition prevents glial inflammasome activation and pyroptosis in models of multiple sclerosis. Proc Natl Acad Sci USA 115:E6065–E6074.

Ozcan U, Yilmaz E, Ozcan L, Furuhashi M, Vaillancourt E, Smith RO, Görgün CZ, Hotamisligil GS (2006) Chemical chaperones reduce ER stress and restore glucose homeostasis in a mouse model of type 2 diabetes. Science 313:1137–1140.

Paganoni S, et al. (2021) Long-term survival of participants in the CENTAUR trial of sodium phenylbutyrate-taurursodiol in amyotrophic lateral sclerosis. Muscle Nerve 63:31–39.

Platnich JM, Chung H, Lau A, Sandall CF, Bondzi-Simpson A, Chen HM, Komada T, Trotman-Grant AC, Brandelli JR, Chun J, Beck PL, Philpott DJ, Girardin SE, Ho M, Johnson RP, MacDonald JA, Armstrong GD, Muruve DA (2018) Shiga toxin/lipopolysaccharide activates caspase-4 and gasdermin D to trigger mitochondrial reactive oxygen species upstream of the NLRP3 inflammasome. Cell Rep 25:1525–1536.e1527.

Rahim RS, St John JA, Crane DI, Meedeniya AC (2018) Impaired neurogenesis and associated gliosis in mouse brain with PEX13 deficiency. Mol Cell Neurosci 88:16–32.

Santos MJ, Quintanilla RA, Toro A, Grandy R, Dinamarca MC, Godoy JA, Inestrosa NC (2005) Peroxisomal proliferation protects from beta-amyloid neurodegeneration. J Biol Chem 280:41057–41068.

Schindelin J, Arganda-Carreras I, Frise E, Kaynig V, Longair M, Pietzsch T, Preibisch S, Rueden C, Saalfeld S, Schmid B, Tinevez JY, White DJ, Hartenstein V, Eliceiri K, Tomancak P, Cardona A (2012) Fiji: an open-source platform for biological-image analysis. Nat Methods 9:676–682.

Sexton JZ, He Q, Forsberg LJ, Brenman JE (2010) High content screening for non-classical peroxisome proliferators. Int J High Throughput Screen 2010:127–140.

Singh I, Paintlia AS, Khan M, Stanislaus R, Paintlia MK, Haq E, Singh AK, Contreras MA (2004) Impaired peroxisomal function in the central nervous system with inflammatory disease of experimental autoimmune encephalomyelitis animals and protection by lovastatin treatment. Brain Res 1022:1–11.

Skon-Hegg C, Zhang J, Wu X, Sagolla M, Ota N, Wuster A, Tom J, Doran E, Ramamoorthi N, Caplazi P, Monroe J, Lee WP, Behrens TW (2019) LACC1 regulates TNF and IL-17 in mouse models of arthritis and inflammation. J Immunol 202:183–193.

Skripuletz T, Bussmann JH, Gudi V, Koutsoudaki PN, Pul R, Moharregh-Khiabani D, Lindner M, Stangel M (2010) Cerebellar cortical demyelination in the murine cuprizone model. Brain Pathol 20:301–312.

Smith JJ, Aitchison JD (2013) Peroxisomes take shape. Nat Rev Mol Cell Biol 14:803–817.

Uzor NE, McCullough LD, Tsvetkov AS (2020) Peroxisomal dysfunction in neurological diseases and brain aging. Front Cell Neurosci 14:44.

Van Camp N, Lavisse S, Roost P, Gubinelli F, Hillmer A, Boutin H (2021) TSPO imaging in animal models of brain diseases. Eur J Nucl Med Mol Imaging 49:77–109.

Vega-Riquer JM, Mendez-Victoriano G, Morales-Luckie RA, Gonzalez-Perez O (2019) Five decades of cuprizone, an updated model to replicate demyelinating diseases. Curr Neuropharmacol 17:129–141.

Vijayan V, Srinu T, Karnati S, Garikapati V, Linke M, Kamalyan L, Mali SR, Sudan K, Kollas A, Schmid T, Schulz S, Spengler B, Weichhart T, Immenschuh S, Baumgart-Vogt E (2017) A new immunomodulatory role for peroxisomes in macrophages activated by the TLR4 ligand lipopolysaccharide. J Immunol 198:2414–2425.

Walker DG, Lue LF (2015) Immune phenotypes of microglia in human neurodegenerative disease: challenges to detecting microglial polarization in human brains. Alzheimers Res Ther 7:56.

Walsh JG, Reinke SN, Mamik MK, McKenzie BA, Maingat F, Branton WG, Broadhurst DI, Power C (2014) Rapid inflammasome activation in microglia contributes to brain disease in HIV/AIDS. Retrovirology 11:35.

Weller S, Gould SJ, Valle D (2003) Peroxisome biogenesis disorders. Annu Rev Genomics Hum Genet 4:165–211.

Yousuf MS, Samtleben S, Lamothe SM, Friedman TN, Catuneanu A, Thorburn K, Desai M, Tenorio G, Schenk GJ, Ballanyi K, Kurata HT, Simmen T, Kerr BJ (2020) Endoplasmic reticulum stress in the dorsal root ganglia regulates large-conductance potassium channels and contributes to pain in a model of multiple sclerosis. FASEB J 34:12577–12598.

Zinnhardt B, Belloy M, Fricke IB, Orije J, Guglielmetti C, Hermann S, Wagner S, Schäfers M, Van der Linden A, Jacobs AH (2019) Molecular imaging of immune cell dynamics during de- and remyelination in the cuprizone model of multiple sclerosis by [(18)F]DPA-714 PET and MRI. Theranostics 9:1523–1537.